Discriminating flint and chert raw materials with LA-ICP-MS/MS, compositional data analysis, and supervised machine learning for archaeological applications

Marie Imbeaux [a,*], Pierre-Yves Collin [b], Fabrice Monna [a], Benoît Caron [c], Rémi Martineau [a], Jehanne Affolter [a,d], Carmela Chateau-Smith [e]

[a] *CNRS, UMR 6298, ARTEHIS, Archéologie Terre Histoire Sociétés, Université Bourgogne Europe, 6 Bd Gabriel 21000 Dijon, France*
[b] *UMR 6282, Biogéosciences, Université Bourgogne Europe, 6 bd Gabriel 21000 Dijon, France*
[c] *UMR 7193, Institut des Sciences de la Terre de Paris (ISTeP), Sorbonne Université, CNRS-INSU, 75005 Paris, France*
[d] *Ar-Géo-Lab, Dîme 86 CH-2000 Neuchâtel, Switzerland*
[e] *UR 4178, CPTC Centre Pluridisciplinaire Textes et Cultures, Université Bourgogne Europe, 4 Bd Gabriel, 21000 Dijon, France*

ARTICLE INFO

ABSTRACT

Identifying lithic production and distribution networks in flint and chert extraction areas is a key issue for better understanding of Neolithic societies. Determining artefact provenance by petrographic characterisation of flint and chert facies is generally efficient, but this method may sometimes be limited by factors such as the opaque white patina that covers many artefacts. This study presents a protocol for geochemical analysis using laser ablation–inductively coupled plasma–tandem mass spectrometry (LA-ICP-MS/MS), compositional data analysis (CoDA), and supervised machine learning (Linear Discriminant Analysis, LDA, Random Forest Leave-One-Out, RFLOO) to complement the petrographic determination of flint and chert sources. The protocol sought to discriminate siliceous raw material exploited in the Saint-Gond Marshes region (SGM; Marne, France) from the Campanian (Ca; Late Cretaceous) and the Bartonian (Ba; Eocene), and flint raw material exploited in the Pays d'Othe region (PO; Aube, France) from the Coniacian (Co; Late Cretaceous). We tested the discrimination potential of geochemical signatures at different spatial (inter- and intra-regional) and stratigraphic scales (Late Cretaceous vs Eocene; Coniacian vs Campanian), formed in different environments (marine vs lacustrine, or within the same sedimentary basin) on a corpus of 52 samples from 9 sites. Our results demonstrate that all three groups are clearly discriminated, as are all but one of the 9 sampling sites. The CoDA procedure transforms raw data into log-ratios discriminated by LDA and RFLOO: the results obtained are more robust than those obtained from the unprocessed raw data. Discrimination is linked to the geochemical and diagenetic processes involved in the formation of flint and chert nodules. Flints and cherts formed in different palaeo-environments will possess distinctive geochemical signatures. These results are very encouraging for sourcing archaeological artefacts, particularly when their provenance cannot be determined petrographically.

1. Introduction

In Europe, flint and chert are present in many sedimentary formations of the Secondary Era (Affolter, 2002; Affolter et al., 2022; Herforth and Alpers, 1980; Hughes et al., 2012; Imbeaux et al., 2018; Jurkowska and Świerczewska-Gładysz, 2020; Tarriño et al., 2015) and Tertiary Era (Bostyn and Lanchon, 1992; Tarriño et al., 2015), but they are not uniformly distributed across territories. During prehistoric times, populations created exchange networks and social connections (Earle and Ericson, 1977) as they distributed siliceous materials from exploitation areas to consumption sites over distances that often remain to be determined. The economic and social organisation of prehistoric societies can be better understood by answering key archaeological questions such as the distribution of flint and chert extraction areas, the source of specialised productions, and the exchange networks between cultural groups (Ericson et al., 1984; Kerig and Shennan, 2015). Among lithic studies, determining the provenance of flint and chert raw materials is less well developed than typology, lithic technology, and use-

---

* Corresponding author.
E-mail address: marie.imbeaux@u-bourgogne.fr (M. Imbeaux).

wear analysis.

Several petrographic and geochemical techniques have been developed to determine the provenance of siliceous raw materials. Among the most common in archaeological studies is the detailed petrographic characterisation of flint and chert nodules (Affolter, 1989; 2002; Affolter et al., 2022; Delvigne et al., 2016; Fabre, 2001; Imbeaux et al., 2018; Masson, 1979, 1981; Séronie-Vivien and Séronie-Vivien, 1987; Valensi 1955; 1957). In such provenance studies, flint and chert facies are defined by detailed descriptions of macroscopic (colour, nodule size, shape, etc.), mesoscopic, and microscopic features. Observations are made at the mesoscopic to the microscopic scale with a stereomicroscope (x10 to x50). Clasts are described in terms of their abundance, diversity, size, fragmentation, and taphonomy. Determining provenance by this method may be limited by three factors: (i) an opaque white patina may partially or even completely cover the artefact or sample, leaving too small a surface area for detailed observations; (ii) small artefacts may present too few discriminating features; (iii) in rare cases, two geographically distant sedimentary formations may present very similar petrographic characteristics.

Another method used to discriminate lithic raw materials is the geochemical analysis of their elemental composition (Andreeva et al., 2014; Bonsall et al., 2010; Brandl et al., 2014, 2016, 2018; Carter and Dussubieux, 2016; Gurova et al., 2016, 2022a, Mauran et al., 2021, 2022; Sanchez Della Torre et al., 2016; Senesi et al., 2023). This method is particularly well suited to the study of volcanic rocks exploited for tool production (e.g., obsidian: Cann and Renfrew, 1964; Costa, 2006; Tykot, 1997; Le Bourdonnec et al., 2010). The distinctive geochemical signature of a volcanic eruption makes such deposits easy to identify even in complex cases (Caron et al., 2023). By contrast, flints and cherts are diagenetic objects contained in sedimentary rocks, where geochemical heterogeneity is generally presumed to be greater than in volcanic rocks. Geochemical fingerprinting can therefore only be considered efficient if intra-deposit heterogeneity is lower than inter-deposit heterogeneity.

Energy dispersive X-Ray Fluorescence (EDXRF) and Portable X-Ray Fluorescence (PXRF) are two non-destructive techniques used to determine the geochemical composition of archaeological flint artefacts (Hughes et al., 2012). For this type of analysis, the surface must be planar, without inclusions or patina, but these conditions are rarely met. Surfaces are almost never completely flat, and inclusions of fossils and grains are very common in siliceous materials, as is patina.

Laser-Induced Breakdown Spectroscopy (LIBS) is a slightly invasive method that can detect chemical elements from a small flint surface (Collin, 2019). In LIBS spectra, concentrations derive from peak intensity. To obtain even semi-quantitative results, the device must be calibrated, which remains challenging. Relative results based on the statistical comparison of averaged spectra have been used to discriminate chert resources to some extent (Senesi et al., 2023).

Inductively Coupled Plasma-Mass Spectrometry (ICP-MS) can be used to quantify many geochemical elements present in flint with high precision (Bressy, 2002; Bruggencate et al., 2018; Garbán et al., 2017; Olofsson and Rodushkin, 2011; Bradley et al., 2020). In liquid mode, the analysis is destructive, as samples are crushed and then totally digested. This complex, costly, time-consuming protocol may be appropriate for raw materials, but unsuitable for valuable archaeological artefacts.

Laser Ablation-Inductively Coupled Plasma-Mass Spectrometry (LA-ICP-MS) can be used to quantify major, minor, and trace geochemical elements with high precision (Andreeva et al., 2014; Bonsall et al., 2010; Brandl et al., 2016, 2018; Gurova et al., 2016, Gurova et al., 2022a,b; Olofsson and Rodushkin, 2011; Moreau et al., 2016, 2019; Petitt et al., 2012; Sanchez Della Torre et al., 2016; Speer, 2014, 2016). This method is therefore particularly suitable for the analysis of flint and chert, as the elements used to define its geochemical signature, apart from silicon, are only present at trace level. Laser ablation causes minimal damage to archaeological artefacts: the smallest laser impact is almost invisible to the naked eye. Thus, even patinated artefacts are analysable if a small pristine surface remains. Flint and chert formed during early diagenesis

(Jurkowska and Świerczewska-Gładysz, 2020, for Cretaceous flint) in different sedimentary contexts can be geochemically and statistically discriminated (Brandl et al., 2016, 2018, Gurova et al., 2016, 2022a,b, Moreau et al., 2016, 2019; Olofsson and Rodushkin, 2011; Petitt et al., 2012; Sanchez Della Torre et al., 2016; Speer, 2014). Some studies have identified geochemical variations within a geological formation (Brandl et al., 2016, 2018; Speer, 2016). Sampling a limited number of outcrops within a formation may not sufficiently take this variability into account, thus preventing the reliable identification of archaeological flint artefact sources (Moreau et al., 2016, 2019; Bradley et al., 2020). Intra-formation geochemical variation has been demonstrated on three outcrops of Edwards Plateau chert in Texas (Speer, 2016), and on five outcrops of "Chocolate silicites" (Jurassic chert in Poland) shown to be discriminable by three geochemical signatures (Brandl et al., 2016).

Our goal in this study was to evaluate whether flint and chert from outcrops in the eastern Paris Basin can be discriminated geochemically. The first step was to develop a sampling protocol for three clearly petrographically discriminated flint and chert groups, of three different ages (i. e. Coniacian, Campanian, and Bartonian), from two different regions (Saint-Gond Marshes vs Pays d'Othe), formed during early diagenesis in different environments (e.g. marine vs lacustrine). Then we developed an analytical protocol based on high-precision LA-ICP-MS/MS analysis (two mass spectrometers in tandem). To evaluate whether flint or chert geochemical signatures can significantly discriminate siliceous raw materials, the data were then processed using compositional data analysis (CoDA) combined with supervised machine learning (i.e. LDA and Random Forest).

2. Archaeological, geographical, and geological context

Two major Neolithic flint and chert extraction areas (not only with pits, but also with deep mining shafts and galleries) only 60 km apart have been identified in the eastern Paris Basin, France (Fig. 1a): the Saint-Gond Marshes region in Marne (Martineau et al., 2019a; Fig. 1b) and the Pays d'Othe region in Aube and Yonne (Augereau, 1995; de Labriffe, 2023; Labriffe et al., 1995; de Labriffe and Thebault, 1995; Fig. 1c). The flints and cherts from these two regions are characterised by different facies (Imbeaux et al., 2018; Affolter and de Labriffe, 2007; Fig. 2). Determining the production networks of these two sectors should provide new information about the technical, economic, and societal organisation of Neolithic populations. Unfortunately, many siliceous artefacts are covered with an opaque white patina, rendering petrographic determination more difficult. High-precision LA-ICP-MS measurements should lead to better determination of the provenance of flint and chert artefacts found in other regions, but potentially sourced from these extraction areas.

2.1. The Saint-Gond Marshes region

The Saint-Gond Marshes region (~80 km^2) is located in the eastern Paris Basin, below an asymmetrical plateau: the Île-de-France cuesta (Fig. 1b). The cuesta slopes and adjacent hills are Campanian Chalk. Tertiary sedimentary formations (clay, sand, sandstone, and limestone) overlie the Chalk at the summits of the plateau and the outlying cuesta remnants (*buttes témoins*). This topography is due to the substantial erosion of the Chalk, which was not protected by Tertiary formations during the Quaternary glaciations and interglacial periods (Hatrival et al., 1988; Depreux et al., 2019). Campanian Chalk contains several flint seams, separated by 5 to 10 m of compact homogeneous chalk. The flint nodules generally measure from 20 to 40 cm in length, although some large irregular slabs may measure up to 1 m in length. The Bartonian cherts are found in lacustrine marls, rich in fossil debris. This seam is discontinuous at the regional scale.

Over 500 Neolithic sites have been identified in the region (Martineau et al., 2014; Martineau et al., 2019a; Edinborough et al., 2021), 36 of which have been excavated: 21 necropolises (with 135
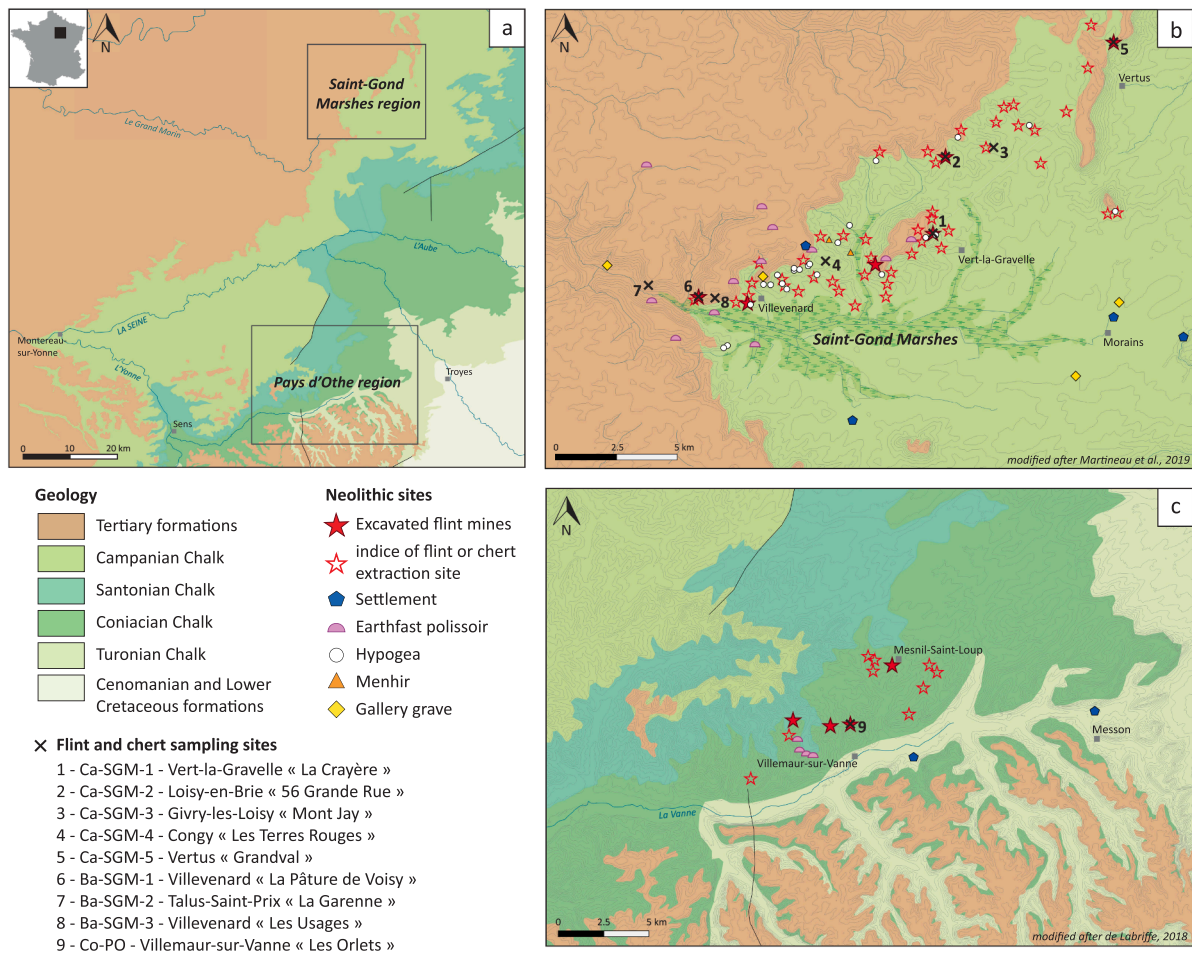
Fig. 1. (a) Geographical and geological context, NE France. (b) Saint-Gond Marshes region, Neolithic sites, flint and chert sampling sites. (c) Pays d'Othe region, Neolithic sites, and sampled flint outcrops. Outcrops are coded as follows: Ca=Campanian, Ba=Bartonian, Co=Coniacian, SGM=Saint-Gond Marshes, PO=Pays d'Othe.

hypogea), 5 gallery graves, 4 settlements, and 6 flint mines (Fig. 1b). Five of the mines exploited Campanian flint (Fig. 2a and b), while the sixth mine exploited Bartonian chert (Fig. 2d and e), with various exploitation techniques (simple extraction pits, quarries with working faces, and shafts with galleries). Pedestrian and aerial surveys have also led to the discovery of at least 43 potential extraction sites (Martineau et al., 2019a; Fig. 1b).

2.2. The Pays d'Othe region

The Pays d'Othe region (~100 km^2; SE Paris Basin) extends on both sides of the Vanne valley (Fig. 1c). Turonian, Coniacian, Santonian, and Campanian chalks form the substratum of the hills, overlain by continental Tertiary sands and sandstones (Pomerol et al., 1981). The flint nodules in the chalk decalcification clays are of poor quality (Pomerol et al., 1981) whereas, at the base of the Coniacian, high-quality flint seams are separated by fractured chalk layers (1–5 m thick). Many of these seams contain numerous small irregular flint nodules (10–20 cm long), while some seams contain larger nodules (30–45 cm). One seam (15–20 cm thick) is an entirely silicified bed (de Labriffe et al., 1995a).

During the archaeological excavations prior to the construction of the A5 highway, four large flint mines were discovered (Augereau, 1995; de Labriffe et al., 1995a, de Labriffe and Thebault, 1995b; de Labriffe, 2023). These excavations documented a major flint extraction area, where knapping workshops produced tens of thousands of flint tools, mainly flint axes, but also flint flakes and irregular blades (Augereau et al, 2021; de Labriffe, 2023). The flint exploitation system

(with shallow pits, shafts, and galleries) was adapted to the slope morphology, specifically targeting the high-quality flint seams present in the stable chalk beds.

Few other sites are known in the Pays d'Othe region, apart from a settlement excavated at Neuville-sur-Vanne, dated from the Middle Neolithic II (Blaser et al., 2017), and another at Messon, dated from the Late Neolithic period (Tsobgou-Ahoupe et al., 2017). Five megalithic collective burials from the Late Neolithic period have been explored, and numerous earthfast polissoirs have been identified (de Labriffe et al., 2018; de Labriffe, 2023).

3. Material and method

3.1. Flint samples

The study seeks to characterise flint and chert sources in three different geological formations, from two regions in the eastern Paris Basin. Nine sampling sites were selected (Table 1): five from the Campanian (Ca-SGM-1 to 5) and three from the Bartonian (Ba-SGM-1 to 3) in the Saint-Gond Marshes region, and one from the Coniacian period (Co-PO) for the Pays d'Othe region. A set of raw siliceous nodules was hammered from each outcrop (maximum: 14, minimum: 3, average: 5; total: 49). For purposes of comparison, three weathered chert slabs from Ba-SGM-1 were also sampled, resulting in a total of 52 samples. Although the flint samples from the five Campanian sites in the Saint-Gond-Marshes region all present the same facies, a different flint subfacies is identified at each site (Appendix A, Appendix B). The three
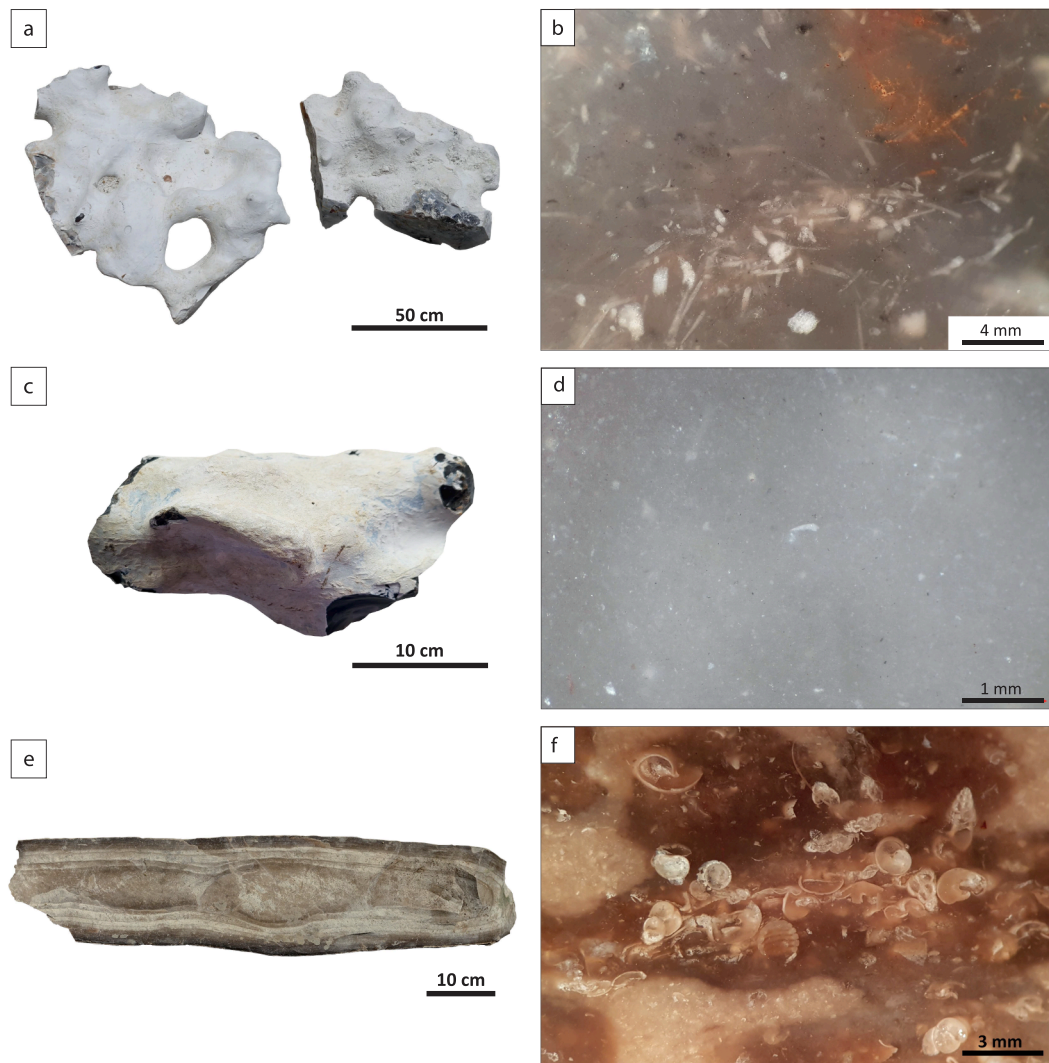
Fig. 2. Chert and flint characteristics. (a) Large irregular slabs of Campanian flint, Saint-Gond Marshes (Ca-SGM-3). (b) Stereomicroscopic image of Campanian flint, Saint-Gond Marshes (Ca-SGM-3). (c) Irregular nodule of Coniacian flint, Pays d'Othe (Co-PO). (d) Stereomicroscopic image of Coniacian flint, Pays d'Othe (Co-PO). (e) Large slab of Bartonian chert, Saint-Gond-Marshes (Ba-SGM-1). (f) Stereomicroscopic image of Bartonian chert, Saint-Gond Marshes (Ba-SGM-1). For outcrop codes, see Fig. 1.

Bartonian sampling sites all present the same chert facies, with no sub-facies variation. The petrographic characteristics of the siliceous materials sampled in both these regions are currently being inventoried in the ARTEHIS rock library (see Fig. 3, in Imbeaux et al., 2018, part of the research programme "Saint-Gond", directed by Rémi Martineau). We also consulted the Ar-Geo-Lab rock library (Neuchâtel, Jehanne Affolter), which documents siliceous rocks throughout the Paris Basin (see Fig. 4, Imbeaux et al., 2018) These rock libraries make it possible to discriminate at basin scale the specific characteristics of the facies described here. Testing geochemical differences in flints and cherts formed in different depositional environments at a regional scale is also possible.

Each sample consists of a nodule (Fig. 3a), broken into flakes (Fig. 3b), from three of which a small fragment or splinter was taken (Fig. 3c). These splinters were taken far from the cortex because the geochemical composition of the cortex and that of the interface between cortex and flint are known to be different from the flint itself (Fernandes et al., 2019). Splinters were selected using a binocular magnifying glass to identify those with the most homogeneous siliceous matrix, i.e., those without figured elements. The splinters were then mounted in epoxy resin (Fig. 3d). Three points were sampled on each splinter by laser ablation (Fig. 3e), resulting in nine values for each of the 30 elements quantified by ICP-MS/MS.

3.2. Analytical protocol

3.2.1. LA-ICP-MS/MS acquisition

Geochemical analysis was carried out in the ALIPP 6 lab, at Sorbonne Université (ISTeP, UMR 7193, OSU Terra UAR 3455, Paris), using a laser ablation system coupled to an inductively coupled plasma tandem mass spectrometer (LA-ICP-MS/MS) Agilent ICP-MS/MS 8800 and 8900, with two mass spectrometers for improved accuracy. Flints were ablated by a 193 nm laser (Laser Photon Machine Analyte G2 Excimer) pulsed at 8 Hz, with a spot size of 130 μm, and a laser power of 5.94 J cm^{-2}. Acquisition time took 1 min for each of the 468 measurements. The 30 elements (major, minor, trace and Rare Earth Elements) were measured on 33 isotopes: ^{23}Na, ^{24}Mg, ^{27}Al, ^{28}Si, ^{39}K, ^{43}Ca, ^{47}Ti, ^{51}V, ^{54}Fe, ^{57}Fe, ^{60}Ni, ^{72}Ge, ^{74}Ge, ^{88}Sr, ^{95}Mo, ^{137}Ba, ^{139}La, ^{140}Ce, ^{141}Pr, ^{146}Nd, ^{147}Sm, ^{153}Eu, ^{157}Gd, ^{159}Tb, ^{163}Tb, ^{163}Dy, ^{165}Ho, ^{166}Er, ^{169}Tm, ^{172}Yb, ^{175}Lu, ^{232}Th, and ^{238}U.

Table 1

Description of the nine sampling sites. Campanian flints from the Saint-Gond Marshes region are coded Ca-SGM-1 to 5, Bartonian cherts from the Saint-Gond Marshes region are coded Ba-SGM-1 to 3, and Coniacian flint from the Pays d'Othe Region is coded Co-PO. (See Appendices A and B for detailed facies and sub-facies descriptions; see Imbeaux et al. 2018 for methodology).

Group code	Sub-group code	GPS (WGS 84)	Village	Site name	Stratigraphy	Sampling sites	Number of samples	Flint and chert facies
Ca-SGM	Ca-SGM-1	48.851655 / 3.893825	Vert-la-Gravelle	La Crayère	Upper Campanian	archaeological excavation (Martineau et al., 2019b)	14	Fine well-sorted sediment. Numerous foraminifera, fragments of sponges, and sponge spicules. Sea urchin spines, bivalves, and brachiopods are rare to common.
Ca-SGM	Ca-SGM-2	48.880085 / 3.903641	Loisy-en-Brie	56 Grande Rue	Upper Campanian	archaeological excavation (Martineau et al., 2012)	4	Fine well-sorted sediment. Numerous micritised foraminifera. Sponge fragments, bivalves, and sea urchin spines are common. Sponge spicules are rare.
Ca-SGM	Ca-SGM-3	48.892335 / 3.931752	Givry-les-Loisy	Mont Jay	Upper Campanian	modern quarry	5	Fine to coarse poorly sorted sediment. Fragmented bioclasts arranged in lamina. Numerous fragments of bryozoan colonies and sea urchin spines. Foraminifera and bivalves are common. Frequent bioturbation.
Ca-SGM	Ca-SGM-4	48.845532 / 3.834146	Congy	Les Terres Rouges	Upper Campanian	modern quarry	3	Fine to coarse poorly sorted sediment. Bryozoan colonies are abundant, with different morphologies (ramified, bifoliate, encrusting). Numerous Foraminifera and sponge spicules. Sponge fragments are common.
Ca-SGM	Ca-SGM-5	48.921341 / 3.998500	Vertus	Grandval	Upper Campanian	outcrop	5	Fine well-sorted sediment with few bioclasts, mainly sponge fragments and spicules, foraminifera, bivalves, and sea urchin spines.
Ba-SGM	Ba-SGM-1	48.829030 / 3.763188	Villevenard	La Pâture de Voisy	Bartonian	archaeological excavation (Martineau et al., 2019b)	8	Very fine to coarse sediment. Concentric opaque and translucent zones in the siliceous matrix. Microbreccia texture, bioturbations, and mudcracks. Bioclasts are mainly gastropods (*Stagnicola longisticatus*, *Planorbina similis*) and Charophyta debris.
Ba-SGM	Ba-SGM-2	48.834880 / 3.734102	Talus-Saint-Prix	La Garenne	Bartonian	outcrop	5	identical to Villevenard "La Pâture de Voisy"
Ba-SGM	Ba-SGM-3	48.828207 / 3.770748	Villevenard	Les Usages	Bartonian	modern quarry	3	identical to Villevenard "La Pâture de Voisy"
Co-PO	Co-PO	48.269643 / 3.725598	Villemaur-sur-Vanne	Les Orlets	Coniacian	archaeological excavation (de Labriffe et al., 1995a)	5	Very fine well-sorted sediment. Foraminifera, echinoids, and sponge fragments are common. All the bioclasts show algal and/or bacterial micritisation (Affolter and de Labriffe, 2007).

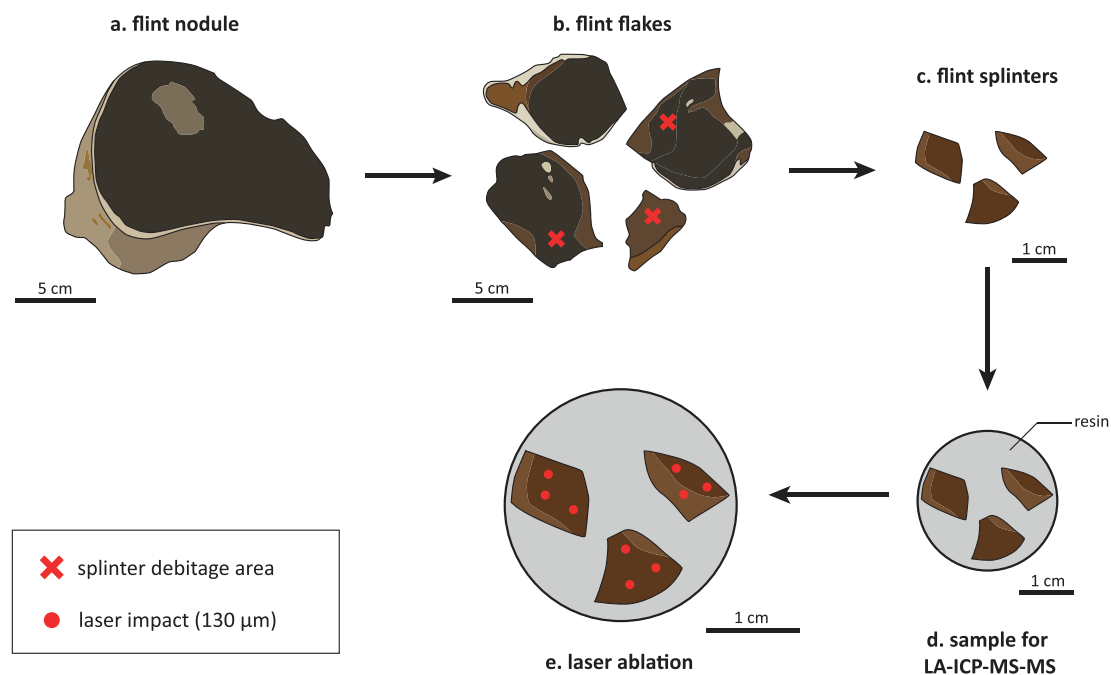**a. flint nodule**   **b. flint flakes**   **c. flint splinters**

5 cm   5 cm   1 cm

d. sample for LA-ICP-MS-MS

resin   1 cm

e. laser ablation

1 cm

✖ splinter debitage area

● laser impact (130 µm)

Fig. 3. Sample preparation protocol.

Fig. 4. Compositional biplot for (a) the three flint and chert groups and (b) the nine sampling sites. The first two axes represent 54.69% and 25.49% of the variance (i.e. 80.12%).

The elements Na, Mg, Al, K, Ca, Ti, Fe, Sr, and Th are classically used to trace continental input in sediments, while the elements V, Mo, Ni, and U, sensitive to redox conditions, are often used to discriminate sedimentary materials (Brumsack, 2006; Tribovillard et al., 2006). The Rare Earth Elements (REE: La, Ce, Pr, Nd, Sm, Eu, Gd, Tb, Dy, Ho, Er, Tm, Yb, and Lu), known to be almost immobile during diagenesis, can be used to trace primary geochemical signatures (Webb and Kamber, 2000; Collin et al., 2015). The Ge/Si ratio can be used to recognize biogenic silica in silicifications (Tribovillard, 2013), while Ba is commonly used to identify variations in primary productivity (Tribovillard et al., 1996).

The LA-ICP-MS/MS was tuned and calibrated through linear scanning of the NIST 612 glass standard at a frequency of 8 Hz and laser fluence of 5.94 J per cm^2. The ICP-MS/MS was used in Tandem mode (Q1 = Q2) with no gas in the collision-reaction cell. The ICP-MS/MS was first tuned to robust plasma conditions, then optimized to minimize oxide production by monitoring the $^{238}U^{16}O/^{238}U$ ratio (here less than 0.015 %). The production of double-charged cations was monitored using $^{44}Ca^{++}$ as a control (44/22 unit mass atomic ratio here less than 2 %). Mass fractionation was limited by monitoring $^{238}U/^{232}Th$ (here always between 1 and 1.1). For standardization and drift correction, the BHVO-2G glass standard was measured after every 2 flint samples.

3.2.2. Data processing

For each run, background noise, with no laser shot, was acquired before and after laser ablation. Linear regression of the background noise was subtracted from the signal. The acquired spectra were carefully examined one by one, and the integration interval was adapted (i. e., reduced) to discard possible analytical spikes due to microlites (e.g., minerals). During acquisition, inclusions and other anomalous phases can be detected in the signal by abnormally high peaks observed in the acquisition spectra. Only the part of the signal corresponding to the siliceous matrix was retained.

The ablated volume may vary over space and time depending on ablation conditions and the type of material analysed. Normalizing all isotopes to an isotope of known composition eliminates this possible analytical bias. Here, ^{28}Si was used for this purpose: the average SiO$_2$ value, previously determined by EPMA (Cameca SX Five, Camparis SU) at the point of analysis, was 99.8 % wtO. The few values below the limit of detection (LOD) were retained for further analysis, as they contain useful information. Values below the LOD were replaced by the LOD divided by the square root of 2 (Baxter, 2003; Camizuli et al., 2014; Hornung and Reed, 1990; Glass and Gray, 2001). The geometric mean

computed from the nine laser measurements obtained from each set of three splinters was used to characterise each flint nodule (Fig. 3).

3.3. Statistical treatments

The fundamentals of compositional data analysis (CoDA) are briefly presented for readers unfamiliar with the concept. More details can be found in the works of Aitchison (1986, 1992) and Barceló-Vidal et al. (2001). Compositional data carry relative information, making absolute values less relevant, focusing instead on the ratios between variables. Let **x** represent a positive vector with D components, a subset of measured concentrations $[x_1,…,x_D]$, summing up to a constant κ, where κ ≤ 1. The vector **x** can be closed to κ = 1 using the closure operation:

$$\mathscr{C}(\mathbf{x}) = \left[\frac{x_1}{\sum_{i=1}^{D}x_i}, \cdots, \frac{x_D}{\sum_{i=1}^{D}x_i}\right]$$

The sample space in CoDA is a simplex S^D, instead of the real space R^D. To address the closed data issue, Aitchison (1986) introduced the centred log-ratio transformation (*clr*), noted as:

$$clr(\mathbf{x}) = \left[ln\frac{x_1}{g_m(\mathbf{x})}, ln\frac{x_2}{g_m(\mathbf{x})}, \cdots, ln\frac{x_D}{g_m(\mathbf{x})}\right]$$

where $g_m(\mathbf{x})$ is the geometric mean of the D parts. Compositional biplots, derived from *clr*-transformed data, allow the structure of compositional datasets to be explored. These biplots represent the relative variation of multivariate datasets by projecting the data on to a plane defined by the first two or three principal components (Aitchison and Greenacre, 2002). Variables are indicated by rays; the link between the apices of two rays approximates their corresponding log-ratio (Aitchison and Greenacre, 2002; Van den Boogaart and Tolosana-Delgado, 2013). In the compositional biplot, interpretations are inherently based on the ratios between all components rather than on individual components analysed separately, as is the case with the classical biplot (Gabriel, 1971). The biplot is used for exploratory data analysis and to identify which log-ratios of variables separate the samples.

Applying multivariate analyses to compare population means is challenging, as the covariance matrix of *clr*-transformed data is always singular. To overcome this issue, Egozcue et al. (2003) developed the *ilr*-transformation (isometric log-ratio), which transforms compositions in the D-part Aitchison simplex into a (D-1) dimensional Euclidean vector. The *ilr*-transformation, given by:

$$ilr(\boldsymbol{x}) = \boldsymbol{z} = [z_1, \cdots, z_{D-1}] \in \mathbb{R}^{D-1}; z_i = \sqrt{\frac{i}{i+1}}ln\sqrt[i]{\frac{\prod_{j=1}^{i}x_j}{x_{i+1}}} \text{ for } i = 1,...., D-1,$$

ensures that the covariance matrix of the *ilr*-transformed dataset is invertible, enabling straightforward application of Multivariate Analysis of Variance (MANOVA) or Linear Discriminant Analysis (LDA) on *ilr*-coordinates (Kovacs et al., 2006). The LDA is a supervised procedure that aims to maximise inter-group variance and minimise intra-group variance to optimise group discrimination.

The Random Forest procedure was also applied to the *ilr*-transformed data. This classification procedure (adapted both to linear and nonlinear problems) builds multiple decision trees using random subsets of data and features. It then combines their predictions to improve accuracy and reduce overfitting. Predictions made by individual decision trees may not be correct, but once the trees have been combined, label predictions will be more accurate and stable (Hastie et al., 2008).

The CoDA approach is particularly appropriate to determine flint or chert composition, as the dominant component in these materials is always silica. Any variation, however small, in the proportion of silica in flint samples will therefore have a drastic impact on all other elemental concentrations. Working with elemental ratios excluding silicon rather than with elemental concentrations should provide more reliable results.

Leave-one-out Cross-Validation (LOO-CV) can be used to evaluate the performance of a machine-learning algorithm (Raschka, 2015). This procedure splits a dataset composed of *n* individuals into a training set and a testing set, using all but one observation as part of the training set. The procedure is then repeated *n* times, leaving out a different sample each time. In our case, the procedure is carried out with an equal prior probability for each group. The cross-validation procedure was used to test the performance of both LDA (LOO-CV) and Random Forest (Random Forest Leave-One-Out, RFLOO).

All the data transformations, operations, and statistical procedures used the R software with the "compositions" (van den Boogaart and Tolosana-Delgado, 2008), "KlaR", "randomforest", "carret", and "ggplot2" packages.

4. Results

4.1. Description of the data

For all three groups (Ca-SGM, Co-PO, and Ba-SGM), Ca is the most abundant element after Si (Table 2; Appendix C; see Appendix D for standard values); it is particularly high in the Ba-SGM group (3930 µg g^{-1}). Mean values for Al, Na, and K are above 100 µg g^{-1} in all three groups, but Al is twice as abundant in Ca-SGM (470 µg g^{-1}), where Fe is also abundant (448 µg g^{-1}). In the Ba-SGM group, Mg is slightly above 100 µg.g^{-1}. Mean values for REEs are always below 1 µg g^{-1}, but the highest values are always found in the Co-PO group. Abnormally high maximum contents were sporadically observed: in the Ca-SGM group, Fe reaches 22900 µg g^{-1}, Ca 23200 µg g^{-1}, and Al 2500 µg g^{-1}; in the Ba-SGM group, Ca reaches 72000 µg g^{-1}. These anomalies may correspond to the laser striking chalk residues, metal oxides, or clay particles.

4.2. Biplots

The *clr*-transformed data are plotted in a compositional biplot for Ca-SGM, Co-PO, Ba-SGM, and the variables, using a form biplot (Fig. 4), as this representation preserves the distances between individuals. The total percentage of variance explained by the first two axes is 80.2 % (54.7 % and 25.5 %). In Fig. 4a, the three groups (Ca-SGM, Co-PO, Ba-SGM) are clearly separated along these axes. The first axis separates the Cretaceous groups (Ca-SGM and Co-PO) from the Eocene cherts (Ba-SGM). It is carried by the log-ratios (Ca, U, Mg, Sr)/ light REE. The second axis separates the two Cretaceous groups, Ca-SGM and Co-PO. It

Table 2
Description of the data acquired by LA-ICP-MS/MS.

		Ti	Al	Fe	Mg	Ca	Na	K	Ge	V	Ni	Sr	Ba	Mo	Th	U
		µg.g^{-1}	µg.g^{-1}	µg.g^{-1}	µg.g^{-1}	µg.g^{-1}	µg.g^{-1}	µg.g^{-1}	µg.g^{-1}	µg.g^{-1}	µg.g^{-1}	µg.g^{-1}	µg.g^{-1}	µg.g^{-1}	µg.g^{-1}	µg.g^{-1}
Ca-SGM	geometric mean	28.2	470	448	17.9	640	466	286	0.365	1.28	0.7	3.45	4.43	0.035	0.099	0.343
	minimum	2.35	178	7.45	7.63	192	200	129	0.044	0.149	0.151	1.3	0.572	0.001	0.013	0.089
	maximum	525	2500	22,900	181	23,200	2090	2870	0.778	43.9	21.3	20	196	0.769	4.315	1.041
Ba-SGM	geometric mean	11.4	198	80.8	121	3930	404	248	0.474	1.18	0.64	22.9	1.72	0.03	0.062	4.23
	minimum	0.198	24.9	15.2	10.9	260	142	74.3	0.237	0.338	0.123	0.555	0.22	0.002	0.007	0.359
	maximum	194	988	544	1730	72,000	909	663	0.882	11.4	2.17	504	8.55	0.523	1.77	37.7
Co-PO	geometric mean	8.3	193	32.5	15.4	838	320	161	0.367	0.331	0.524	2.93	0.645	0.028	0.053	0.287
	minimum	0.734	110	17.4	6.66	439	158	102	0.256	0.159	0.3	1.46	0.338	0.006	0.025	0.167
	maximum	25.4	332	71.7	38.3	4770	777	237	0.548	0.835	1.48	8.67	1.35	0.158	0.228	0.454

		La	Ce	Pr	Nd	Sm	Eu	Gd	Tb	Dy	Ho	Er	Tm	Yb	Lu
		µg.g^{-1}	µg.g^{-1}	µg.g^{-1}	µg.g^{-1}	µg.g^{-1}	µg.g^{-1}	µg.g^{-1}	µg.g^{-1}	µg.g^{-1}	µg.g^{-1}	µg.g^{-1}	µg.g^{-1}	µg.g^{-1}	µg.g^{-1}
Ca-SGM	geometric mean	0.408	0.392	0.105	0.377	0.082	0.028	0.0976	0.021	0.081	0.025	0.052	0.014	0.04	0.014
	minimum	0.041	0.031	0.009	0.0356	0.005	0.002	0.001	0.002	0.007	0.001	0.003	0.0003	0.005	0.001
	maximum	7.76	5.92	1.61	6.49	1.34	0.326	1.57	0.231	1.28	0.287	0.737	0.102	0.464	0.118
Ba-SGM	geometric mean	0.079	0.144	0.033	0.069	0.026	0.015	0.026	0.013	0.026	0.015	0.022	0.013	0.023	0.012
	minimum	0.005	0.006	0.004	0.005	0.004	0.001	0.002	0.0001	0.003	0.001	0.001	0.0002	0.001	0.001
	maximum	0.867	0.985	0.316	0.702	0.15	0.084	0.131	0.074	0.128	0.095	0.098	0.086	0.085	0.072
Co-PO	geometric mean	0.831	0.6	0.207	0.685	0.146	0.048	0.163	0.039	0.133	0.044	0.087	0.022	0.067	0.022
	minimum	0.282	0.205	0.082	0.134	0.05	0.021	0.057	0.021	0.051	0.021	0.03	0.01	0.036	0.01
	maximum	2.12	1.4	0.486	1.62	0.329	0.102	0.388	0.076	0.33	0.078	0.193	0.06	0.142	0.06

is essentially carried by the log-ratios of the detrital elements (Al, Fe, Ti, Ba, Ge, K, Na, V, Th)/heavy REE. In Fig. 4b, where each outcrop is identified by a different colour, the projection along the first two axes separates the outcrop sub-groups to some extent, suggesting that applying further statistical analysis (LDA and Random Forest) should allow each outcrop sub-group to be discriminated.

4.3. LDA, RFLOO, and confusion matrices

Linear Discriminant Analysis (LDA) is applied to the ilr-transformed data to test whether the groups can be discriminated. As expected, the projection of flints on the first two canonical variables (CV1 and CV2; Fig. 5a) allows the three groups to be discriminated. The LOO-CV procedure was then applied to evaluate LDA performance more formally, resulting in a confusion matrix (Table 3). For the three groups, only two of the 52 samples are misclassified (~96 % accuracy). For the nine sampling sites, seven of the site clusters are clearly separated, with only two data points from the Ca-SGM-4 sub-group overlapping the Ca-SGM-1 sub-group (Fig. 5b). In the confusion matrix (Table 4), there are no classification errors for five of the sites, and only ten of the 52 samples are misclassified (~80 % accuracy), five of which are from Ca-SGM-1, the subgroup with the most samples.

Applying the RFLOO procedure to the *ilr*-transformed data improved all the results, as shown by the confusion matrices (Tables 5 and 6). For the three groups, only one of the 52 samples is still misclassified (Table 5 vs Table 3). For the nine sampling sites, only seven of the 52 samples are still misclassified (Table 6 vs Table 4). The results are proportionally better for the sub-groups with the largest number of samples, but there is still one misclassified sample for each of the BA-SGM sub-groups.

To quantify the improvement achieved through the CoDA procedure, we also applied LDA to the raw data, where the results for the sampling sites were much less satisfactory (see Appendix E). The comparative F-values obtained by MANOVA (ilr-transformed data vs raw data) decreased from 20 to 12 for the three groups, and from 12 to 5 for the nine sampling sites.

5. Discussion

5.1. Validating protocols and statistical analyses

Discrimination with LDA (Fig. 5), LOO-CV (Table 3), and RFLOO (Table 5) is validated at the scale of the group. At the sampling site scale, despite the similarity of sedimentological and diagenetic conditions within each group during early diagenesis, discrimination is possible for most of the sites. This result demonstrates the efficiency of the proposed protocol: (*i*) sampling five nodules per outcrop, (*ii*) taking measurements

Table 3
Confusion matrix for the ilr-transformed data of the three flint and chert groups. The prior probability is 1/3 each group (accuracy: 0.9615).

		groups		
		Ca-SGM	**Co-PO**	**Ba-SGM**
predicted groups	**Ca-SGM**	30	–	1
	Co-PO	1	5	–
	Ba-SGM	–	–	15

directly in the siliceous matrix without impurities, (*iii*) taking splinters from three different points in the flint nodule, and (*iv*) averaging LA-ICP-MS/MS measurements for each flint or chert nodule. In this geological context, with this protocol, sampling multiple nodules per outcrop is no longer necessary for clear geochemical characterisation (thus saving time and financial resources during field missions, sample management, and analyses).

Our results confirm that flints and cherts from different geological formations can be discriminated, as previously shown for different geological periods on flints or cherts diagenetically formed in marine sediments (Brandl et al., 2016, 2018; Moreau et al., 2016, 2019). Our protocol also discriminates between Eocene cherts and Cretaceous flints formed in lacustrine and marine sediments.

Transforming raw data into log-ratios overcomes such slight variation, as the inter-elemental ratios become the only data of interest. Setting silica concentration at 99.8 % is no longer of primary importance. A value of 99.9 % would reduce the raw concentration of all the remaining elements by half, but would have no effect on the ratios, so that results using LDA or RFLOO would remain the same.

When the sum of all components is equal to 100 % (i.e. any chemical composition), no component can vary independently from the others. With this closure constraint, spurious correlations are expected, particularly if a predominant element (e.g., SiO_2) varies, even slightly. Multivariate statistics based on correlation or covariance matrices (e.g., PCA or LDA) should not be applied to raw data. In the most favourable situations, the performance of statistical analyses will deteriorate with standard PCA or LDA, as observed here. In other circumstances, the consequences may be more serious, leading to erroneous conclusions. Linear correlations between elements may be observed because the silica content is not stable within the set of samples studied, thus masking discrimination potential. The novel use of compositional biplots applied here to flint characterisation can overcome this problem. The projection of the *clr*-transformed data can reveal the dispersion of samples, indicating which sets of log-ratios of elements are involved in group separation.
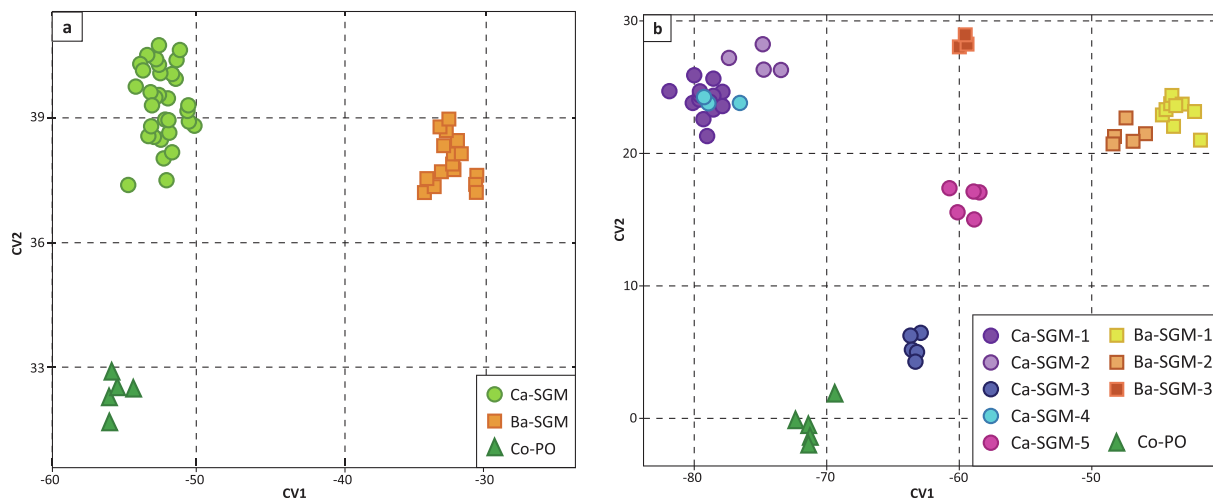

Fig. 5. Results for LDA on ilr-transformed data for the three groups (a) and for the nine sampling sites (b).

Table 4
Confusion matrix for the ilr-transformed data of the flint and chert sampling sites. The prior probability is 1/9 for each group (accuracy: 0.8076).

		sub-groups (sampling sites)								
		Ca-SGM-1	Ca-SGM-2	Ca-SGM-3	Ca-SGM-4	Ca-SGM-5	Ba-SGM-1	Ba-SGM-2	Ba-SGM-3	Co-PO
predicted groups	Ca-SGM-1	9	1	–	–	–	–	–	–	–
	Ca-SGM-2	2	3	–	–	–	–	–	–	–
	Ca-SGM-3	–	–	5	–	–	–	–	–	–
	Ca-SGM-4	3	–	–	3	–	–	–	1	–
	Ca-SGM-5	–	–	–	–	5	1	–	–	–
	Ba-SGM-1	–	–	–	–	–	5	–	–	–
	Ba-SGM-2	–	–	–	–	–	2	5	–	–
	Ba-SGM-3	–	–	–	–	–	–	–	2	–
	Co-PO	–	–	–	–	–	–	–	–	5

Table 5
Confusion matrix of the RFLOO results applied to the ilr-transformed data of the three flint and chert groups (accuracy: 0.9808).

		groups		
		Ca-SGM	Co-PO	Ba-SGM
predicted groups	Ca-SGM	31	–	1
	Co-PO	–	5	–
	Ba-SGM	–	–	15

5.2. Palaeo-environmental interpretation of flint and chert geochemical signatures

In the compositional biplot (Fig. 4), the log-ratios of the chemical elements with ray apices close to each other are almost constant (e.g., Ca/U, Na/K, or Lu/Tm). Conversely, the further apart the ray apices, the more the log-ratios vary (e.g., Ca/La, Fe/Tm, or Al/Mo). With constant or quasi-constant log-ratios, it is assumed that the variations of the elements concerned are associated with similar geochemical processes, whether sedimentary or diagenetic. Three groups of clr-transformed elements can be identified. The first is composed of Ba, K, Fe, Al, Ti, V, Na, Ge, and Th, the second is composed of Ca, Sr, Mg, and U, and the third is composed of the REEs. The elements in the first group are associated with bottom detrital flows in sedimentary basins. When found together, the elements in the second group generally indicate an evaporitic continental sedimentary domain, concentrated by lake-water evaporation. The Ca/Mg log-ratio may be linked to dolomite formation in an evaporitic context, while strontium is a marker of watershed erosion in the continental domain (Feïss et al., 2004). Uranium content can be linked to detrital flows or to the preservation of organic matter. Here the distance between the log-ratios of U and the elements in the first group rules out detrital flows. High U content is associated here with high organic matter content, as observed in lacustrine sediments (Spirakis, 1996).

The REEs forming the third group are strongly influenced by detrital flow and precipitation conditions in sedimentary deposits. These much less mobile elements are less affected by late diagenesis and can be used

to trace the chemical conditions that prevailed during deposition and early diagenesis (Kamber and Webb, 2001). Examples of averaged Post-Archean Australian Shale (PAAS)-normalized REE patterns (McLennan, 1989) are presented in Fig. 6. The patterns for the two sets of Cretaceous samples (Campanian, Fig. 6a; Coniacian, Fig. 6b) indicate porewater with a negative Ce anomaly characteristic of open marine depositional environments (Murray, 1994; Olofsson and Rodushkin, 2011; Piper and Bau, 2013). The Bartonian REE patterns (Fig. 6c) have relatively flat profiles, with a slight enrichment in heavy REEs, typical of alkaline salt-lake environments (Johannesson et al., 1994a; Johannesson et al., 1994b). The results obtained in this study are consistent with current sedimentological and palaeogeographic knowledge (Gély and Hanot, 2014; Guillocheau et al., 2000).

The flints and cherts in this study archive information about the geochemical composition of the porewater in sediments just below the water/sediment interface and thus provide information about the depositional environment. Geochemical analysis can therefore be used not only to discriminate between basin types (marine vs continental), but also at outcrop scale within the same basin. Inter-group discrimination is supported by sets of elements and not merely by one specific element. The porewater geochemistry recorded during flint or chert formation can be measured using LA-ICP-MS/MS and differences in geochemical signatures can be identified using compositional statistics.

5.3. Archaeological applications of LA-ICP-MS vs petrographic analysis of flint artefacts

The results from this study demonstrate that Bartonian (Eocene) cherts can be differentiated from Cretaceous flints by geochemical analysis, based on CoDA and supervised machine learning (LDA, RFLOO). A clear geochemical distinction is also observed between the Campanian flint from the Saint-Gond Marshes region and the Coniacian flint from the Pays d'Othe region (Fig. 5, Tables 3 and 4), thus potentially allowing the region of flint or chert extraction to be identified in a corpus of archaeological artefacts. The Saint-Gond Campanian flint facies can be divided by petrographic analysis into five sub-facies, thus discriminating the five outcrops sampled. These sub-facies were also clearly differentiated by statistical geochemical analysis (Fig. 5b),
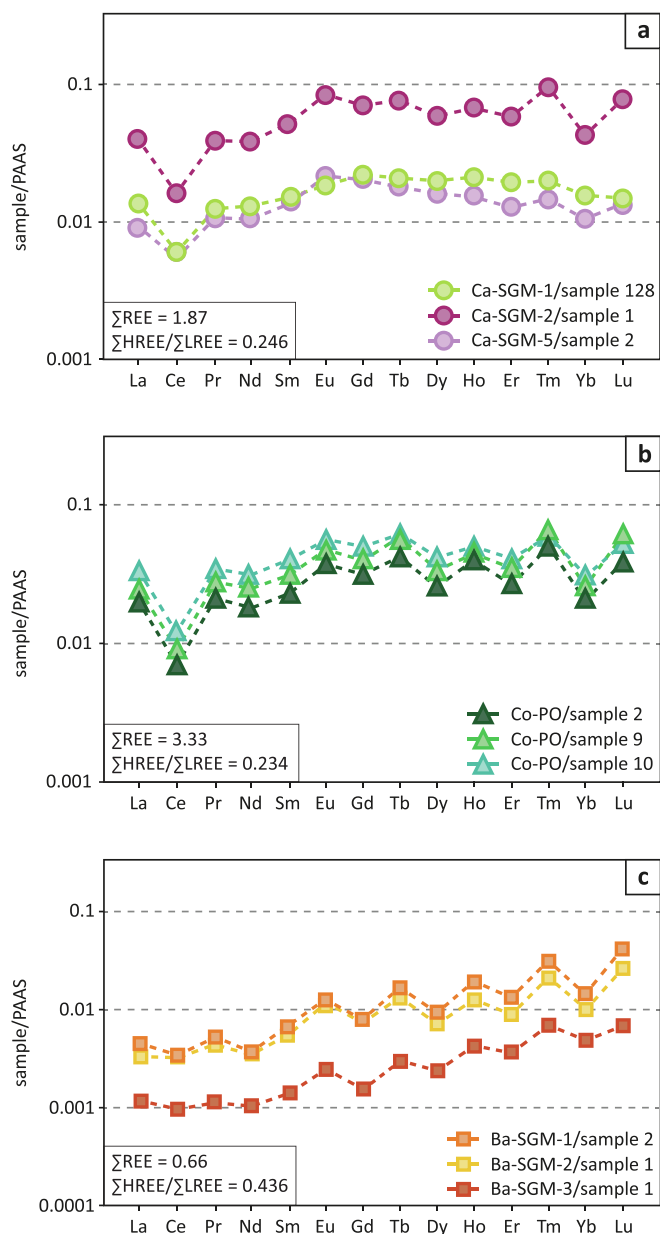
Table 6
Confusion matrix of the RFLOO results applied to the ilr-transformed data of the flint and chert sampling sites (accuracy: 0.865).

		sub-groups (sampling sites)								
		Ca-SGM-1	Ca-SGM-2	Ca-SGM-3	Ca-SGM-4	Ca-SGM-5	Ba-SGM-1	Ba-SGM-2	Ba-SGM-3	Co-PO
predicted sub-groups	Ca-SGM-1	14	2	–	1	–	–	–	1	–
	Ca-SGM-2	–	2	–	–	1	–	–	–	–
	Ca-SGM-3	–	–	5	–	–	–	–	–	–
	Ca-SGM-4	–	–	–	2	–	–	–	–	–
	Ca-SGM-5	–	–	–	–	4	–	–	–	–
	Ba-SGM-1	–	–	–	–	–	7	1	–	–
	Ba-SGM-2	–	–	–	–	–	1	4	–	–
	Ba-SGM-3	–	–	–	–	–	–	–	2	–
	Co-PO	–	–	–	–	–	–	–	–	5

Fig. 6. Averaged patterns of PAAS-normalized REE values with sampling site code/sample number. (a) Campanian flints from the Saint-Gond Marshes region (Ca-SGM); (b) Coniacian flints from the Pays d'Othe region (Co-PO); (c) Bartonian cherts from the Saint-Gond Marshes region (Ba-SGM). ∑REE: averaged REE values; ∑HREE/∑LREE: ratio between averaged heavy and light REE values.

except for the overlap between Ca-SGM-1, with 14 samples, and Ca-SGM-4, with only 3 samples. To improve discrimination and reduce Type 2 error, the recommended number of samples should therefore be increased to at least five.

The LDA results for the Eocene cherts clearly indicate that the three outcrops can be discriminated by geochemical analysis. As the three outcrops are from the same facies with no discernible sub-facies, statistical geochemical analysis is more efficient than petrographic determination.

Results from an earlier study of patinated Cretaceous flint artefacts from Spiennes (Moreau et al., 2016) suggest that the non-weathered part of the artefacts presents a similar geochemical signature to that of flints taken directly from outcrops. In this study, three patinated flint slabs from Villevenard "La Pâture de Voisy" were analysed in the same way as

the five outcrop samples (Ba-SGM-1). Care was taken to sample a non-patinated zone within these slabs, which had lain on the ground for many years. As the LDA placed all eight samples in the same cluster (Fig. 5b), and as the samples are also well attributed in confusion matrices (Tables 4 and 6), it is considered that the geochemical signature of the slabs remained unaffected by weathering. To confirm this hypothesis, future studies should focus on the analysis of a sufficient number of patinated archaeological artefacts to allow the statistical methods presented here to be used.

These geochemical analyses should prove useful when sourcing typological pieces that cannot be determined by their facies, either because they have too much patina or because they have too few discriminating components, which is often the case with very small artefacts. It is essential to build databases of geochemical signatures for flint and chert sources, with a broad spectrum of facies. Supervised machine learning is a powerful tool to discriminate the origin of artefacts when all potential sources have been catalogued, as the reliability of the protocol is directly related to the accurate identification and characterisation of siliceous lithic sources. Several studies have pointed out that intra-formation variability must be fully characterised to allow reliable artefact sourcing (Bradley et al., 2020; Moreau et al., 2016, 2019). This study demonstrates the reliability of the protocol with three petrographically distinct flint and chert groups from the Paris Basin. It is also effective for the nine sub-groups (outcrops) where the petrographic differences are less obvious. The protocol is validated for the detection of intra-formation variability, with multiple analyses on a minimum of five samples per outcrop for optimal results.

The exhaustive sampling preceding the application of the protocol is both expensive and time-consuming. Such sampling has been carried out in the Saint-Gond marshes region for at least ten years (Imbeaux et al., 2018). A similar project is underway in the Pays d'Othe region and throughout the eastern part of the Paris Basin. This project should provide a representative rock library for the eastern Paris Basin, a necessary step before building a database populated by geochemical analyses. It is also essential to identify all the flint and chert extraction sites exploited during the Neolithic period in these territories. These limitations are not specific to siliceous raw materials; the same difficulties apply to archaeological investigations of copper sourcing based on lead isotopes (e.g., around the Mediterranean; Artioli et al., 2020). Elemental geochemistry, like isotope geochemistry, determines geochemical compatibility between raw materials and outcrops rather than the direct identification of sources.

6. Conclusions

Cretaceous (Campanian) flints and Eocene (Bartonian) cherts from the Saint-Gond Marshes region (Marne, France) and Cretaceous (Coniacian) flints from the Pays d'Othe region (Aube, France) were analysed by LA-ICP-MS/MS, and the results were processed by compositional data analysis (CoDA) and a supervised machine-learning procedure (LDA, RFLOO). In the eastern Paris Basin, major Neolithic flint and chert extraction areas have already been identified in both these regions (de Labriffe, 2023; Martineau et al., 2019a). The protocol implemented to compare the geochemical signatures of siliceous raw materials from these regions yields convincing results. The three petrographically distinguishable flint and chert groups can also be discriminated by their geochemical signatures. Cretaceous flints from different outcrops sharing the same facies but different sub-facies provide evidence of subtle lateral variations in the depositional environment (e.g., water and porewater chemistry, detrital flows, organic matter content, etc.) recorded during early diagenesis (Jurkowska and Świerczewska-Gładysz, 2020). These siliceous raw materials can therefore be discriminated both geochemically and petrographically.

This study demonstrates that the geochemical signature varies less within a flint or chert nodule, or even within an outcrop, than at the scale of a region or between regions. Facies determination is a non-

destructive method that can be routinely applied to siliceous materials and most of the archaeological artefacts in a corpus. The LA-ICP-MS/MS method complements petrographic analysis by the geochemical characterisation of siliceous raw materials. It particularly useful in the case of typological artefacts that cannot be sourced by facies analysis alone.

These initial results demonstrate the importance of combining petrographic and geochemical studies to characterise flint or chert sources. The provenance of the raw materials used to produce archaeological artefacts can be determined by combining petrographic, geochemical, and archaeological (lithic typology and technology) data to identify distribution networks for tools, blanks, and other artefacts in Neolithic mining regions. Sourcing siliceous raw materials can only be successful when all the extraction areas have been categorised; the workflow presented here should contribute to this goal.

CRediT authorship contribution statement

Declaration of competing interest

The authors declare that they have no known competing financial interests or personal relationships that could have appeared to influence the work reported in this paper.

Acknowledgements

Appendix A. Supplementary material

Supplementary data to this article can be found online at https://doi.org/10.1016/j.jasrep.2025.105084.

Data availability

Data are given in supplementary material

References

Affolter, J., 1989. Première approche des gîtes de silex et de leur exploitation préhistorique, in: S. Graeser (Ed.) Mineria Helvetica. Bulletin de la société suisse d'histoire des mines, 9/1989, 55-60.

Affolter, J., 2002. Provenance des silex préhistoriques du Jura et des régions limitrophes. Archéologie neuchâteloise n°28, Neuchâtel, Service et Musée cantonal d'archéologie, 2 volumes.

Affolter, J., de Labriffe, P.-A., 2007. « Mais où sont passées les haches en silex ? ». in: M. Besse (Ed.), Sociétés Néolithiques, des faits archéologiques aux fonctionnements socio-économiques, Actes du 27e colloque interrégional sur le Néolithique

(Neuchâtel 1-5 octobre oct. 2005), Lausanne. Cahier d'archéologie romande, 108, 13-22.

Affolter, J., Wehren, H., Emmenegger, L., 2022. Determination method of silicites (siliceous raw materials): an explanation based on four selected raw materials. Quarter. Int. 615, 33–42.

Aitchison, J., 1986. The Statistical Analysis of Compositional Data. Chapman and Hall, London.

Aitchison, J., 1992. On criteria for measures of compositional difference. Math. Geol. 24, 265–379.

Aitchison, J., Greenacre, M., 2002. Biplots of compositional data. J. Royal Statist. Soc.: Series C (Appl. Statist.) 51, 375–392.

Andreeva, P., Stefanova, E., Gurova, M., 2014. Chert raw materials and artefacts from NE Bulgaria: a combined petrographic and LA-ICP-MS study. J. Lithic Stud. 1 (2), 25–45. https://doi.org/10.2218/jls.v1i2.1129.

Augereau, A., 1995. Les ateliers de fabrication de haches de la minière du Grand Bois Marot à Villemaure-sur-Vanne (Aube), Les mines de silex au Néolithique en Europe occidentale. Actes de la table ronde internationale, Vesoul, 18-19 octobre 1991, 145-158.

Augereau, A., Bostyn, F., Hauzeur, A., Imbeaux, M., de Labriffe, P.-A., Martineau, R., Affolter, J., 2021. L'exploitation du silex au Néolithique dans le Pays d'Othe (Aube) et les Marais de Saint-Gond (Marne) : des systèmes d'extraction à la diffusion des produits. L'aube, Un Espace Clé Sur Le Cours De La Seine, Actes Du Colloque Arkéaube 58–72.

Barceló-Vidal, C., Martin-Fernandez, J., V. Pawlowsky-Glahn, V., 2001. Mathematical foundations of compositional data analysis. Proceedings of IAMG.

Baxter, M., 2003. Statistics in archaeology. Arnold, London.

Blaser, R., Brunet, P., Irribaria, R., Marti, F., Bayle, G., Paresys, C., Giros, R., Mazière, T., Lemunier, S., sur Vanne, N., 2017. Rue du Mont-Royal Occupations néolithiques et protohistoriques sur la rive gauche de la Vanne. Rapport de fouille, Inrap.

Bostyn, F., Lanchon, Y., 1992. In: Jablines Le Haut Chàteau (Seine-et-Marne). Une minière de silex au Néolithique, Documents d'archéologie française, p. 35.

Bonsall, C., Gurova, M., Hayward, C., Nachev, Ch., Pearce, N.J.G., 2010. Characterization of 'Balkan flint' artefacts from Bulgaria and the Iron Gates using LA-ICP-MS and EPMA. Int. Stud. XXII-XXIII, 9–18.

Bradley, S., Cummings, V., Baker, M.J., 2020. Sources of flint in Britain and Ireland: a quantitative assessment of geochemical characterisation using acid digestion inductively coupled plasma-mass spectrometry (ICP-MS). J. Archaeol. Sci.: Rep. 31, 102281.

Brandl, M., Hauzenberg, C., Postl, W., Martinez, M.M., Filzmoser, P., Trnka, G., 2014. Radiolarite studies at Krems-Wachtberg (Lower Austria): Northern Alpine versus Carpathian lithic resources. Quarter. Int. 351, 146–162.

Brandl, M., Hauzenberg, C., Martinez, M.M., Filzmoser, P., Werra, D.H., 2016. The Application of the Multi-Layered Chert Sourcing Approach (MLA) for the Characterisation and Differntiation of "Chocolate Silicites" from Holy Cross Mountains, South-Central Poland. Archaeologica Austriaca 100, 119–149.

Brandl, M., Martinez, M.M., Hauzenberger, C., Filzmoser, P., Nymoen, P., Mehler, N., 2018. A multi-technique analytical approach to sourcing Scandinavian flint: Provenance of Ballast flint from the shipwreck "Leirvigen 1" Norway. PLoS ONE, e0200647.

Bressy, C., 2002. Caractérisation et gestion du silex des sites mésolithiques et néolithiques du Nord-Ouest de l'arc alpin. Une approche pétrographique et géochimique. Unpublished PhD thesis, Université Aix-Marseille I, https://www.theses.fr/2002AIX10025.

ten Bruggencate, R.E., Milne, S.B., Mostafa, F., Park, R.W., Stenton, D.R., Hamilton, A.C., 2018. Characterizing southern Baffin Island chert: A cautionary tale for provenance research. J. Archaeol. Sci.: Rep. 22, 324–329.

Brumsack, H.J., 2006. The trace metal content of recent organic carbon-rich sediments: Implications for Cretaceous black shale formation. Palaeogeography, Palaeoclimatology, Palaeoecology 232, 344–361.

Cann, J.R., Renfrew, C., 1964. The characterization of obsidian and its application to the Mediterranean region. Proc. Prehistoric Soc. 30, 111–133.

Caron, B., Del Manzo, G., Villemant, B., Bartolini, A., Moreno, E., Le Friant, A., Bassinot, F., Baudin, F., Alves, A., 2023. Marine records reveal multiple phases of Toba's last volcanic activity. Scient. Rep. 13, 11575.

Carter, A.K., Dussubieux, L., 2016. Geologic provenience analysis of agate and carnelian beads using laser-ablation-inductively coupled plasma-mass spectrometry (LA-ICP-MS): A case study from Iron Age Cambodia and Thailand. J. Archaeol. Sci.: Rep. 6, 321–331.

Camizuli, E., Monna, F., Scheifler, R., Amiotte-Suchet, P., Losno, R., Beis, P., Bohard, B., Chateau, C., Alibert, P., 2014. Impact of trace metals from past mining on the aquatic ecosystem: a multi-proxy approach in the Morvan (France). Environ. Res. 134, 410–419.

Collin, J. P., 2019. De la mine à l'habitat : Économie des productions minières du Bassin de Mons au Néolithique. De la fin du 5e millénaire à la fin du 3e millénaire avant notre ère. Unpublished PhD thesis, Université de Namur et Université Paris 1 – Panthéon-Sorbonne.

Collin, P.Y., Kershaw, S., Tribovillard, N., Forel, M.B., Crasquin, S., 2015. Geochemistry of post-extinction microbialites as a powerful tool to assess the oxygenation of shallow marine water in the immediate aftermath of the end-Permian mass extinction. Int. J. Earth Sci. 104, 1025–1037.

Costa, L.J., 2006. Récents acquis sur la circulation préhistorique de l'obsidienne en Corse. Bulletin De La Société Préhistorique Française 103 (1), 71–85.

Delvigne, V., Fernandes, P., Piboule, M., Lafarge, A., Raynal, J.P., 2016. Circulation de géomatières sur de longues distances au Paléolithique supérieur: le cas du silex Turonien du Sud du Bassin parisien. C. R. Palevol 16, 82–102.

Depreux, B., Quiquerez, A., Bégeot, C., Camerlynck, C., Walter-Simonnet, A.-V., Ruffaldi, P., Martineau, R., 2019. Small headwater stream evolution in response to Lateglacial and Early Holocene climatic changes and geomorphological features in the Saint-Gond marshes (Paris Basin, France). Geomorphology 345, 106830.

Earle, T.K., Ericson, J.E., 1977. Exchange systems in Prehistory. Academic Press, London.

Edinborough, K., Martineau, R., Dufraisse, A., Shennan, S., Imbeaux, M., Dumontet, A., Schauer, P., Cook, G., 2021. A Neolithic population model based on new radiocarbon dates from mining, funerary and population scaled activity in the Saint-Gond Marshes region of North East France. Quarter. Int. 586, 121–132.

Egozcue, J., Pawlowsky-Glahn, V., Mateu-Figueras, G., Barceló-Vidal, C., 2003. Isometric log-ratio transformations for compositional data analysis. Math. Geol. 35, 279–300.

Ericson, J.E., Ericson, J.E., Purdy, B.A., 1984. Toward the analysis of lithic production systems. In: Prehistoric quarries and lithic production. Cambridge University Press, pp. 1–9.

Fabre, J., 2001. L'économie du silex dans la moyenne vallée de la Somme au Néolithique final : l'exemple de la minière d'Hallencourt et des sites périphériques. Revue archéologique de Picardie, 3-4-2001, 5-80.

Feïss, C., Bonté, P., Andrieu, A., Lefevre, I., 2004. Transfert de matières des bassins versants côtiers au milieu marin : identification, caractérisation et vitesse. L'exemple de la baie du Marin (Martinique). Géomorphologie : Relief, Processus, Environnement 10–1, 81–90.

Gabriel, K.R., 1971. The biplot-graphic display of matrices with application to principal component analysis. Biometrika 58, 453–467.

Garbán, G., Martínez, M., Márquez, G., Rey, O., Escobar, M., Esquinas, N., 2017. Geochemical signatures of bedded cherts of the upper La Luna Formation in Táchira State, western Venezuela: Assessing material provenance and paleodepositional setting. Sedimentary Geol. 347, 130–147.

Gély, J.-P., Hanot, F., 2014. Le Bassin de parisien, un nouveau regard sur la géologie. Bull. Inf. Géol. Bass. Paris, mémoire hors-série 9.

Glass, D.C., Gray, C.N., 2001. Estimating mean exposures from censored data: exposure to benzene in Australian petroleum industry. Ann. Occup. Hyg. 45, 275–282.

Guillocheau, F., Robin, C., Allemand, P., Bourquin, S., Brault, N., Dromart, G., Friedenberg, R., Garcia, J.P., Gaulier, J.M., Gaumet, F., Grosdoy, B., Hanot, F., Le Strat, P., Mettraux, M., Naplas, T., Prijac, C., Rigollet, C., Serrano, O., Grandjean, G., 2000. Meso-Cenozoic geodynamic evolution of the Paris Basin: 3D stratigraphic constraints. Geodinamica Acta 13, 189–246.

Gurova, M., Andreeva, P., Stefanova, E., Stefanov, Y., Kocic, M., Boric, D., 2016. Flint raw material transfers in the prehistoric lower Danube Basin: an integrated analytical approach. J. Archaeol. Sci.: Rep. 5, 422–441.

Gurova, M., Andreeva, P., Stefanova, E., Aladzhov, A., Bonsall, C., 2022b. Petrographic and geochemical analyses of flint raw materials from Bulgaria: a reliable combination for provenance studies of archaeological flint. Quat. Int. 615, 18–32. https://doi.org/10.1016/j.quaint.2021.03.023.

Hatrival, J. N., Chertier, B., Morfaux, P., 1988. Notice explicative de la feuille Montmort au 1/50 000. Edition B.R.G.M., Orléans.

Gurova, M., Stefanova, E., Andreeva, P., Kecheva, K., Bonsall, C., 2022a. Prehistoric flint raw materials and artefacts from Bulgaria: The next step in provenancing Balkan flint. Archaeologia Bulgarica XXVI. 3, 1–30.

Hastie, T., Tibshirani, R., Friedman, J., 2008. The elements of statistical learning. Springer.

Herforth, A., J. Alpers, J., 1980. Geologische Grundlagen des Feuersteinbergbaus in Europa. In: Weisgerber, Weiner (Ed.), 5000 Tausend Jahre Feuersteinbergbau-Die Suche nach dem Stahl der Steinzeit. Bochum, Veröffentlichungen aus dem Bergbaumuseum, 77, 14-16.

Hornung, R.W., Reed, L.D., 1990. Estimation of average concentration in the presence of nondetectable values. Appl. Occup. Environ. Hyg. 5, 46–51.

Hughes, R.E., Högberg, A., Olausson, D., 2012. The chemical composition of some archaeologically significant flint from Denmark and Sweden. Archaeometry 54–55, 779–795.

Imbeaux, M., Affolter, J., Martineau, R., 2018. Diffusion du silex crétacé des minières de Saint-Gond (Marne, France) au Néolithique récent et final. Bulletin De La Société Préhistorique Française 115 (4), 733–767.

Johannesson, K.H., Berry Lyons, W., Bird, D.A., 1994. Rare earth element concentrations and speciation in alkaline lakes from the western U.S.A. Geophys. Res. Lett. 21 (9), 773–776.

Johannesson, K.H., Berry Lyons, W., 1994. The rare earth element geochemistry of Mono Lake water and the importance of carbonate complexing. Limnol. Oceanograp. 39 (5), 1141–1154.

Jurkowska, A., Świerczewska-Gładysz, E., 2020. Evolution of Late Cretaceous Si cycling reflected in the formation of siliceous nodules (flint and cherts). Global Planetary Change 195, 1–26.

Kamber, B.S., Webb, G., 2001. The geochemistry of late Archean microbial carbonate: implications for ocean chemistry and continental erosion history. Geochim. Cosmochim., Acta 65, 2509–2525.

Kerig, T., Shennan, S., 2015. Connecting networks. Characterising contact by measuring lithic exchange in the European Neolithic. Archaeopress Archaeology Oxford.

Kovacs, J., Kovacs, G., Martín-Fernández, J., Barceló-Vida, C., 2006. Major-oxide compositional discrimination in Cenozoic volcanites of Hungary. Geol. Soc. London Special Publications 264, 11–23.

Labriffe, P.-A., Augereau, A., Sidéra, I., Ferdouel, F., 1995. Villemaur-sur-Vanne « Les Orlets » (Aube), quatrième et dernière minière de l'autoroute A5. Résultats préliminaires. Revue Archéologique De Picardie 105–119.

de Labriffe, P.-A., Thebault, D., 1995. Mines de silex et grands travaux : l'autoroute A5 et les sites d'extraction du Pays d'Othe, in : J. Pelegrin et A. Richard (Eds.), Les mines de silex en Europe : avancées récentes. Actes de la table ronde internationale de Vesoul, 18-19 octobre 1991. Paris, CTHS, Documents Préhistoriques, 7, 47-66.

de Labriffe, P.-A., 2018. Mines de silex néolithiques en Pays d'Othe. in: N. Dohrmann et V. Riquier (Eds.), Archéologie dans l'Aube, des premiers paysans au prince de Lavau, 5300 à 450 avant notre ère. Troyes, Gand, Snoeck, 108-111.

de Labriffe, P.-A., 2023. « Les Orlets » and « Le Grand Bois Marot » at Villemaur-sur-Vanne (Aube, France) : face to face in the Pays d'Othe mining complex. In: Bostyn, F., Lech, J., Saville, A., Werra, D.H. (Eds.), Prehistoric Flint Mines in Europe. Archéopress, Oxford, pp. 407–422.

Le Bourdonnec, F.-X., Bontempi, J.-M., Marini, N., Mazet, S., Neuville, P.F., Poupeau, G., Sicurani, J., 2010. SEM-EDS characterization of western Mediterranean obsidians and the Neolithic site of A Fuata (Corsica). J. Archaeol. Sci. 37, 92–106.

Martineau, R., Dumontet, A., Charpy, J.-J., Laplaige, C., Bossuet, G., Affolter, J., Dupont, A., Jacottey, L., Thevenot, J.-P., Stock, A., Lambot, B., 2012. Les habitats néolithiques dans les marais de Saint-Gond. Prospection thématique. Sondage à Morains-le-Petit. In: « Le Canal », « La Fosse à Gérard », « Les Vordes ». Fouilles de Loisy-en-Brie « 56 Grande Rue ». Rapport d'opérations archéologiques.

Martineau, R., Charpy, J.-J., Affolter, J., Lambot, B., 2014. Les minières de silex néolithiques des marais de Saint-Gond (Marne). Revue Archéologique De L'est 63, 25–45.

Martineau, R., Imbeaux, M., Affolter, J., Charpy, J.-J., Bostyn, F., Dumontet, A., 2019a. The Neolithic Flint Mines of Les Marais de Saint-Gond and La Côte des Blancs (Marne, France), in: H. Collet and A. Hauzeur (Eds.), Mining and Quarrying. Geological Characterisation, Knapping Processes and Distribution Networks during Pre- and Protohistoric Times, Proceedings of the 7th International Conference of the UISPP Commission on Flint Mining in Pre- and Protohistoric Times, Mons and Spiennes (Belgium), 28 sept. 1st oct. 2016. Anthropologica et Praehistorica, 128. Bruxelles: SRBAP, 101-118.

Masson, A., 1979. Recherches sur la provenance des silex préhistoriques, méthode d'étude, Etudes Préhistoriques. Revue Régionale D'archéologie Préhistorique 15, 29–40.

Masson, A., 1981. Pétroarchéologie des roches siliceuses, intérêts en préhistoire. Université de Lyon. Unpublished PhD thesis.

Mauran, G., Caron, B., Détroit, F., Nankela, A., Bahain, J.-J., Pleurdeau, D., Lebon, M., 2021. Data pretreatment and multivariate analyses for ochre sourcing: application to Leopard Cave (Erongo, Namibia). J. Archaeol. Sci.: Rep. 35, 102757.

Mauran, G., Caron, B., Beck, L., Détroit, F., Noûs, C., Tonbret, O., Pleurdeau, D., Bahain, J.-J., Lebon, M., 2022. Standardization procedure to provide a unified multi-method elemental compositional dataset, application to ferruginous colouring matters from Namibia. J. Archaeol. Sci.: Rep. 43, 103454.

McLennan, S.M., 1989. Rare Earth Elements in sedimentary rocks: influence of provenance and sedimentary processes. Rev. Mineral. Geochem. 21 (1), 169–200.

Moreau, L., Brandl, M., Filzmoser, P., Hauzenberger, C., Goemaere, E., Jadin, I., Collet, H., Hauzeur, A., Schmitz, R.W., 2016. Geochemical sourcing of flint artefacts from western Belgium and German Rhineland: Testing hypotheses on Gravettian Period mobility and raw material economy. Geoarchaeol.: Int. J. 31, 229–243.

Moreau, L., Ciornel, A., Gjesfjeld, E., Filzomer, P., Gibson, S.A., Day, J., Nigst, P.R., Noiret, P., Macleod, R.A., Niţ, L., Anghelinu, M., 2019. First geochemical "fingerprint" of Balkan and Prut flint from Paleolithic Romania: potentials, limitations, and future directions. Archeometry 61 (3), 521–528.

Murray, R.W., 1994. Chemical criteria to identify the depositional environment of chert: general principles and applications. Sediment. Geol. 90 (3-4), 213–232. https://doi.org/10.1016/0037-0738(94)90039-6.

Piper, D.Z., Bau, M., 2013. Normalized rare earth elements in water, sediments and wine: identifying sources and environmental redox conditions. Am. J. Analy. Chem. 4, 69–83.

Olofsson, A., Rodushkin, I., 2011. Provenancing flint artefacts with ICP-MS using REE signatures and Pb isotopes as discriminants: preliminary results of a case study from northern Sweden. Archaeometry 53–56, 1142–1170.

Petitt, P., Rockman, M., Chenery, S., 2012. The British Final Magdalenian: Society, settlement and raw material movements revealed through LA-ICP-MS trace element analysis of diagnostic artefacts. Quat. Int. 272–273, 275–287.

Martineau, R., Affolter, J., Bostyn, F., Charpy, J.-J., Collin, P.-Y., Desmeulles, J., Dumontet, A., Granjon, L., Huard, P., Imbeaux, M., Lépine, G., Pillot, L., 2019b. Les minières de silex de Vert-la-Gravelle (Vert-Toulon) « La Crayère » et de Villevenard « La Pàture de Voisy » (Marne). Prospections gîtologiques du silex du sud-ouest de la Marne. Rapport de programme de prospection thématique 2019.

Pomerol, B., Monciardini, C., Chateauneuf, J.-C., Farjanel, G., Bournerias, M., Tomasson, R., Tourenq, J., Mégnien, F., 1981. Notice explicative de la feuille d'Estissac au 1/50 000. B.R.G.M., Orléans.

Raschka, S., 2015. Python machine learning, Second edition. Packt Publishing.

Sanchez Della Torre, M., Bourdonnec, F.-X., Gratuze, B., Domingo, R., Garcià-Simon, L. M., Montes, L., Utrilla, P., 2016. Applying ED-XRF and LA-ICP-MS to geochemically characterize chert: the case of the Central-Eastern Pre-Pyrenean lacustrine cherts and their presence in the Magdalenian of NE Iberia. J. Archaeol. Sci.: Rep. 13, 88–98.

Senesi, G.S., Allegretta, I., Marangoni, B.S., Ribeiro, M.C.S., Porfido, C., Terzano, R., De Pascale, O., Eramo, G., 2023. Geochemical identification and classification of cherts using handheld laser induced breakdown spectroscopy (LIBS) supported by supervised machine learning algorithms. Appl. Geochem. 151, 1056256.

Séronie-Vivien, R.-M., Séronie-Vivien, M., 1987. Les silex du Mésozoïque nord- aquitain, Supplément au Bulletin de la Société Linnéenne de Bordeaux, tome XV.

Speer, C.A., 2014. Experimental sourcing of Edwards Plateau chert using LA-ICP-MS. Quat. Int. 342, 199–213.

Speer, C.A., 2016. A comparison of instrumental techniques at differentiating outcrops of Edwards Plateau chert at the local scale. J. Archaeol. Sci.: Rep. 7, 389–393.

Tarriño, A., Elorrieta, I., García-Rojas, M., 2015. Flint as raw material in prehistoric times: cantabrian mountain and western pyrenees data. Quat. Int. 364, 94–108.

Tribovillard, N.P., Caulet, J.P., Vergnaud-Grazzini, C., Moureau, N., Tremblay, P., 1996. Lack of organic matter accumulation on the upwelling influenced Somalia margin in a glacial-interglacial transition. Marine Geol. 133 (3–4), 157–182.

Tribovillard, N., Algeo, T.J., Lyons, T.W., Riboulleau, A., 2006. Trace metals as paleoredox and paleoproductivity proxies: An update. Chemical Geol. 232, 12–32.

Tribovillard, N., 2013. The Ge/Si ratio as a tool to recognize biogenic silica in chert. Compt. Rendus. Geosci. 345, 160–165.

Tsobgou-Ahoupe, R., Dandurand, G., Bandelli, A., Jacottey, L., Fronteau, G., Brunet, P., Irribaria, R., Desiderio, A.-M., Houget, E., Aubazac, G., Bionaz V., Bergantz, F., Jeannès, A., Giros, R., Bigot, J.-J., 2017. Gazoduc "Arc de Dierrey", Zone 24 : Une occupation de la Transition Néolithique moyen-Néolithique récent, Grand-est, Aube, Messon, « Le Longues Royes », Rapport de fouille archéologique, Inrap.

Tykot, R.H., 1997. Characterization of Monte Arci (Sardinia) Obsidian Sources. J. Archaeol. Sci. 24, 467–479.

Valensi, L., 1955. Etude micropaléontologique des silex du magdalénien de St Amand. Bulletin De La Société Préhistorique Française 52 (9-10), 584–597.

Valensi, L., 1957. Micropaléontologie des silex du Grand-Pressigny. Bulletin De La Société Géologique De France, Paris 6, 1083–1090.

van den Boogaart, K.G., Tolosana-Delgado, R., 2008. "compositions": A unified R package to analyze compositional data. Comp. & Geosci. 34–4, 320–338.

van den Boogaart, K.G., Tolosana-Delgado, R., 2013. Analyzing Compositional Data With R. Springer.

Webb, G., Kamber, B.S., 2000. Rare earth elements in Holocene 432 reefal microbialites: A new shallow seawater proxy. Geochim. Cosmochim. Acta 64, 1557–1565.